Busse Balloon for Optical Frequency Combs From a Semiconductor Laser With Time-Delayed Optoelectronic Feedback

Md Shariful Islam, A. Kovalev, G. Danilenko, E. Viktorov, D. Citrin, Alexandre Locquet

Busse Balloon for Optical Frequency Combs from a Semiconductor Laser with Time-delayed Optoelectronic Feedback

Md Shariful Islam *Member, IEEE*, A.V. Kovalev, G.O. Danilenko, E.A. Viktorov, D.S. Citrin, and A. Locquet

***Abstract*—We propose a new mechanism for the generation of optical frequency combs (OFCs) in a semiconductor laser with nonlinear time-delayed optoelectronic feedback. We demonstrate, theoretically and experimentally, that a highly stable periodic regime exists in a closed region of the parameter space known as the Busse balloon. The boundary of the balloon is formed by the secondary Hopf bifurcation. The observed periodic regime results in a >30 GHz bandwidth OFC with microwave spacing between lines and a nearly parabolic distribution of narrow 10-20 MHz linewidths.**

***Index Terms*—Semiconductor Laser, Optoelectronic feedback, Optical combs.**

I. Introduction

Optical frequency combs (OFCs) are crucial in applications ranging from high-precision spectroscopy [1], [2] and precision measurements [3], to broadband laser-based gas sensing [4], molecular fingerprinting [5], and telecommunications. This research area within photonics has been extensively explored over the past decade. Generating low-jitter, tunable, wide-band, and integrable OFCs with microwave line spacings is fundamental for developing a range of modern technologies. Popular platforms for ultrastable wideband OFC generation include microresonators [6]–[8], mode-locked fiber lasers [9], VCSELs [10], [11], and gain modulation of optical amplifiers [12], though these approaches frequently require complex setups for comb stabilization.

Microresonators are among the primary candidates for OFC generation; a continuous-wave pump laser interacts with an ultrahigh-Q microresonator via a Kerr nonlinearity to produce equidistant optical lines in [6]. Recent studies have expanded OFC generators' capabilities, demonstrating designs that meet the needs of 200 GHz spaced WDM data transmission systems and offer ultrawide, tunable OFC generation [7], [8]. Besides microresonators, passively mode-locked fiber lasers have been optimized to produce stable OFCs [9]. VCSELs and other semiconductor laser diodes (LDs) have also been explored for OFC generation, with the gain-switching mechanism playing a key role [10], [11], [13].

Md Shariful Islam, D.S. Citrin, and A. Locquet are with Georgia Tech-CNRS IRL 2958, Georgia Tech–Europe, 2 Rue Marconi, 57070 Metz, France and the School of Electrical and Computer Engineering, Georgia Institute of Technology, Atlanta, GA 30332-0250 USA. e-mail: david.citrin@ece.gatech.edu.

A.V. Kovalev, G.O. Danilenko and E.A. Viktorov are with ITMO University, Birzhevaya Liniya 14, 199034 Saint Petersburg, Russia. e-mail: avkovalev@niuitmo.ru.

The link between OFCs and microwave frequency combs (MFCs) has been examined, highlighting OFC technology's interdisciplinary impact [3], [14]. Experimental stabilization and measurement of OFCs relative to MFCs are documented in [3], while theoretical exploration of timing jitter's impact on both combs is presented in [14].

Semiconductor LDs are attractive for OFC generation because of their compactness, low cost, and high efficiency. A number of techniques has been proposed to produce OFCs with LDs, and in particular gain switching [15], [16], electro-optic modulation [17], mode-locking [18], and micro-ring resonators [19] have contributed to the success of LDs for OFC generation. With gain switching, short pulses are produced when operating the laser close to threshold and coherence is achieved through optical injection or feedback. In the case of external modulation, broad combs can be obtained whose characteristics depend on the modulators used. Mode-locking and micro-ring resonators provide wide combs but the repetition rate, determined by the cavity, cannot be tuned. We report here for the first time an OFC resulting from the operation of a LD, subjected to optoelectonic (OE) feedback, in a parameter region, called a Busse balloon, where highly stable periodic oscillations occur.

More specifically, LDs with OE feedback exhibit a rich variety of dynamical regimes, some of which are of interest for applications, including in microwave photonics. The broad array of usage for this technology, especially in optical communications [20], high-precision spectroscopy [21], and molecular fingerprinting [22], is revealed by numerous works exploring subharmonic, frequency-locked, and chaotic states with both positive and negative OE feedback [23]–[27]. In particular, Ref. [28] demonstrates the generation of a MFC based on a LD with negative feedback, which can be stabilized through an external microwave modulation. Our recent work [29] reported on MFC generation via gain-switching in a semiconductor LD with OE feedback, although the lack of power near the laser threshold left optical characterization incomplete. That is, in that report we were unable to determine if the production of the MFCs was accompanied by OFC generation.

In the present work, we investigate *positive* OE feedback producing OFCs with up to 30 GHz bandwidth in a regime where undamped natural oscillations are known to dominate the dynamics. Although this bandwidth seems limited for OFCs compared to more mature technologies, the robustness of OE systems against environmental and experimental

disturbances as well as their compactness and potential for integration are noteworthy. The pulse-to-pulse phase locking is induced by the time-delayed feedback. The ability of such systems to generate OFCs may open new applications for these combs. On a relevant note, we have reported staircase-like switching in a *negative* OE feedback case for the RF and optical spectra in [30]. The optical spectrum for an injection current J close to twice the threshold current J_{th} is composed of equidistant lines that are separated by a few GHz and give rise to an OFC. In the current *positive* OE feedback case, we have reported MFCs in [29] where both the gain-switched and relaxation-oscillation regimes are shown to produce MFCs with equidistant RF lines. In this feedback type, the output of the LD with OE feedback is an optical pulse train whose repetition rate is the inverse of the OE feedback loop time delay τ.

This article aims to build upon foundational works [10], [31] and advance the field of OFCs in the context of microwave photonics by offering a novel perspective on OFC generation through semiconductor LDs with OE feedback. The rest of the article is organized as follows: Section II reviews the experimental setup. In Sec. III we present the results and discussion, while in Sec. IV we conclude.

II. Experiment

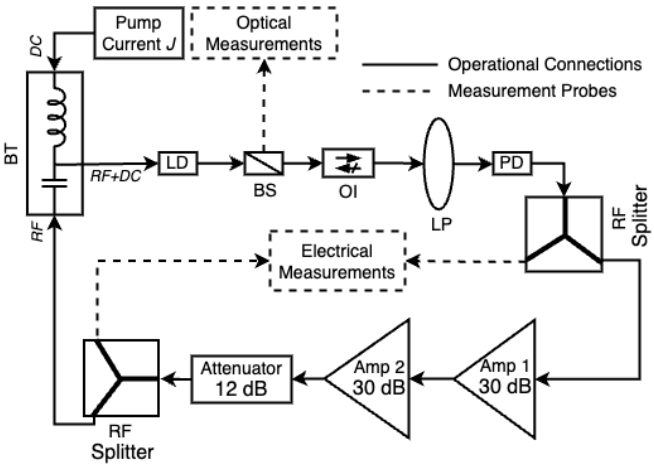

Fig. 1. Experimental setup. BS: beam splitter, BT: bias tee, LD: laser diode, CL: collimating lens, OI: optical isolator, LP: linear polarizer, FC: fiber coupler, PD: photodetector, Amp: amplifier. OI is inserted to prevent any back reflection to LD, and LP is placed to control the feedback strength. The feedback signal originates from PD and is amplified before feeding it to the microwave input arm of BT for modulating the injection current. Electrical measurements are performed after PD and after the attenuator, whereas the optical spectrum is monitored with BS just after LD.

In this experiment, we use an unpackaged edge-emitting multi-quantum well LD operating at wavelength 1550 nm. This LD is a single-mode device featuring a distributed feedback structure built on an InGaAsP/InP strained-layer substrate. Its front facets are coated with an antireflection layer, which contributes to its low beam divergence. As an unpackaged coherent light source, it provides the flexibility needed to adjust the carrier population through either external or self-induced feedback mechanisms. Prior to the experiments, we ensured the optical components are precisely aligned and the LD is thermally stabilized using a Thorlabs TED200C temperature controller. The LD is powered by a controlled current source (Thorlabs LDC201CU), and has a threshold current J_{th} of 20 mA and an external slope efficiency of 0.22 mW/mA, as specified in the LD's datasheet. Figure 1 illustrates our experimental setup, further details of which, including device model numbers, can be found in [32].

The LD output is split in two, with one segment directed to an Aragon Photonics BOSA-200C spectrum analyzer for optical-spectrum analysis (optical resolution: 0.08 pm/10 MHz, wavelength accuracy: ±0.5 pm, and scanning speed: 20 nm/s), and the other used for the feedback loop and optical intensity monitoring. This feedback loop is initiated by channeling the divided output through an optical isolator (OI), which suppresses undesired reflections back into the LD. Subsequently, the light passes through a linear polarizer (LP), positioned before of the photodetector (PD), to fine-tune the feedback intensity. The signal from the PD undergoes amplification via two 30-dB amplifiers (Microsemi UA0L30VM–30 GHz) arranged in series, which is preceded by a 12-dB attenuator (Minicircuits BW-S6W2+, DC–18 GHz) and subsequently routed through a bias tee (BT, with a bandwidth of 10 MHz–26.5 GHz) into the LD injection terminals. The DC branch of the BT receives the current J, while the feedback signal is input into the AC branch. Notably, the PD's low-noise amplifier, along with the OE loop's two 30-dB amplifiers, are inverting, thus constituting a negative feedback signal. The LD's common anode configuration results in a negative voltage at the injection point, resulting in a system with overall *positive* feedback.

We quantify feedback strength by the mean square current fed back into the LD injection terminals, normalized to the DC current in an open-loop scenario, as elaborated in [30]. Throughout these experiments, the feedback strength was fixed at 26% by maintaining the fixed angle ϕ between the LP and the direction of polarization of the laser, so 70% of the light passed through the LP. We observed that higher feedback strengths led to increased linewidth of the OFC teeth, while lower strengths reduced the comb bandwidth. The feedback loop's total delay is $\tau = 10.78$ ns, determined by propagating a periodic pulse train via the BT's AC arm and observing the output from the electronic branch in an open-loop configuration. The feedback loop's bandwidth is confined between 10 MHz and 12 GHz, restricted on the lower end by the BT and on the upper end by the PD's operational limits. The Microsemi amplifiers' maximum saturated output power is 23 dBm.

III. Results and Discussion

In this section, we describe our experiments on the generation, optimization, and characterization of the OFCs. Figure 2 displays radio frequency (RF) spectrographs as a function of J, with the magnitude of the spectra illustrated via the colorbar. In other words, at each J, we measure the optical-intensity time series $I(t)$ and record its Fourier transform. The highest peak at each J is highlighted with a red dot, while the

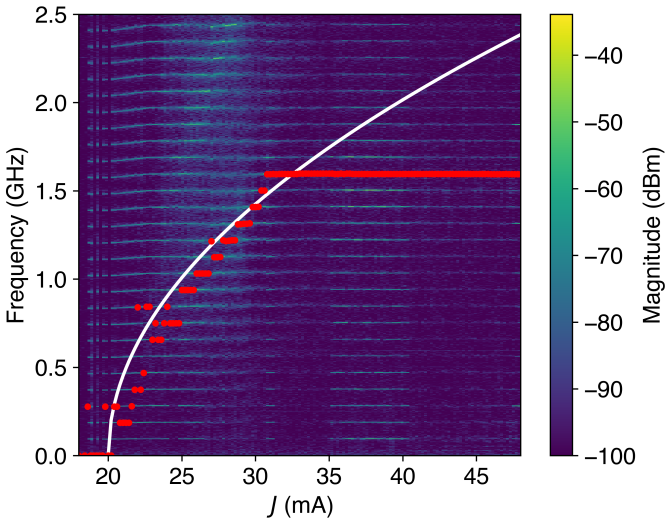

Fig. 2. RF spectrograph of the LD intensity by varying J; maxima are highlighted in red at each J. The white curve is the trend of the relaxation-oscillation frequency of the solitary LD scaled by half.

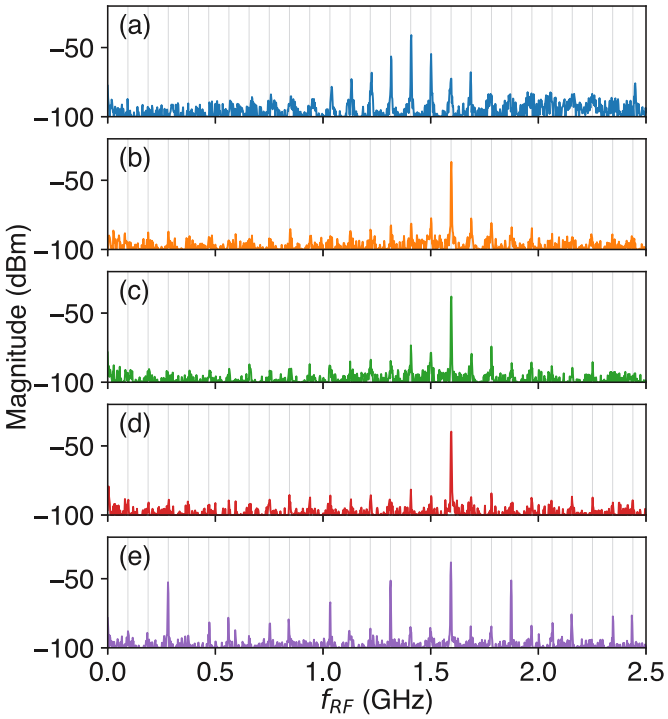

Fig. 3. Examples of RF spectra from different parts of the Busse region in Fig. 2 (flat red line) at the following values of J: (a) 30.2 mA; (b) 43 mA; (c) 45 mA; (d) 47 mA; (e) 48 mA. (a) and (e) exhibit characteristics of quasi-periodic limit cycles, as demonstrated by the secondary oscillations around the main spectral peak. (b–d) display regular periodic limit cycles.

white line represents half the relaxation-oscillation frequency f_{RO} of the solitary laser. It has been previously reported that the pulsing frequency in *positive* OE feedback is one half of the f_{RO} [25] and our current findings are consistent with this observation. Our group has previously reported on different regimes of this OE feedback scheme which corresponded to gain-switched and frequency-locked states producing optical pulse trains (MFCs) and optical square waves [29], [33], [34]. The current experiment utilizes a slightly lower feedback delay of $\tau = 10.78$ ns which is found to be more favorable to high-performance OFC generation compared to earlier setups discussed in [29], [34]. For $J \leq 30$ mA, the maximum spectral peak generally aligns with $\sqrt{J - J_{th}}$, while from 30 to 48 mA, the LD oscillates at a fixed frequency of ~ 1.60 GHz (1.5976 GHz to be precise), gradually transitioning through various dynamical states. Near the boundaries of the constant frequency region denoted by a flat horizontal red line, the RF spectra exhibit quasi-periodic (QP) characteristics interspersed with regular periodic (RP) states. This region of constant frequency regular pulsations bounded by quasiperiodic dynamics is known as Busse balloon [35], [36].

Figure 3 shows examples of RF spectra within the stable frequency region shown in Fig. 2. We highlight two instances of QP limit cycles at $J = 30.2$ and 48 mA, and three RP limit cycles at $J = 43$, 45, and 47 mA. The QP cycles are characterized by secondary oscillation frequencies that modulate around the primary spectral peaks at ~ 1.60 GHz. In contrast, the RP limit cycles exhibit single dominant peaks at the same frequency. The focus of this figure is within the 0–2.5 GHz range, yet it should be noted that the RP limit cycles consist of equidistant RF lines. In all cases shown, the RF spectra consist of a narrow peak, which indicates that the timing of the pulses is well-locked due to the time-delayed feedback.

Optical spectra in Fig. 4 reveal the development of OFCs taken at the same J as in Fig. 3. The broadest OFC spans over 30 GHz, featuring eighteen equidistant teeth at 1.5958 GHz intervals measured at least over 10-dB from the noise floor. The RP states generate superior OFCs compared to the QP states, with a more parabolic spectral distribution and finer comb teeth. QP states, exhibiting secondary frequencies around each primary peak, may be unsuitable for OFC applications.

The OFCs in the RP regime show narrow peaks while the QP OFCs show broader lineshapes. This indicates that the *optical* phase may wander over the duration of the measurement even though the timing of the pulses is locked by the feedback.

By adjusting J while keeping η constant at 0.7, we optimized the OFC production in the range of $2.2J_{th}$ to $2.4J_{th}$. Figure 5(a) illustrates the OFC measured from the output of the free-running LD. The OFC with its 3-dB full-width-at-half-maxima (FWHM) linewidths exhibits a maximum near the edges, with the central peaks being narrower than those at the extremes, ranging from 21 MHz to 10 MHz, constrained by the 10 MHz resolution bandwidth of the spectrum analyzer. Figure 5(b) in the RP regime between $J = 43$ mA and 48 mA illustrates the deviation in comb line intervals from their mean, defined as $\sigma_{OS} = \mathrm{STD}[\Delta f_{OS} - \langle \Delta f_{OS} \rangle]$, where $\langle \cdots \rangle$ represents frequency averaging and Δf_{OS} denotes the intervals between the comb teeth. Notably, σ_{OS} is less than 15 MHz in most cases. Experimental limitations such as thermal fluctuations, alignment precision, and noise in the electronic components prevent the achievement of higher-quality combs.

To provide insight into the theoretical mechanism behind the stable OFC generation, we use a model of a single-mode semiconductor LD subject to filtered nonlinear OE

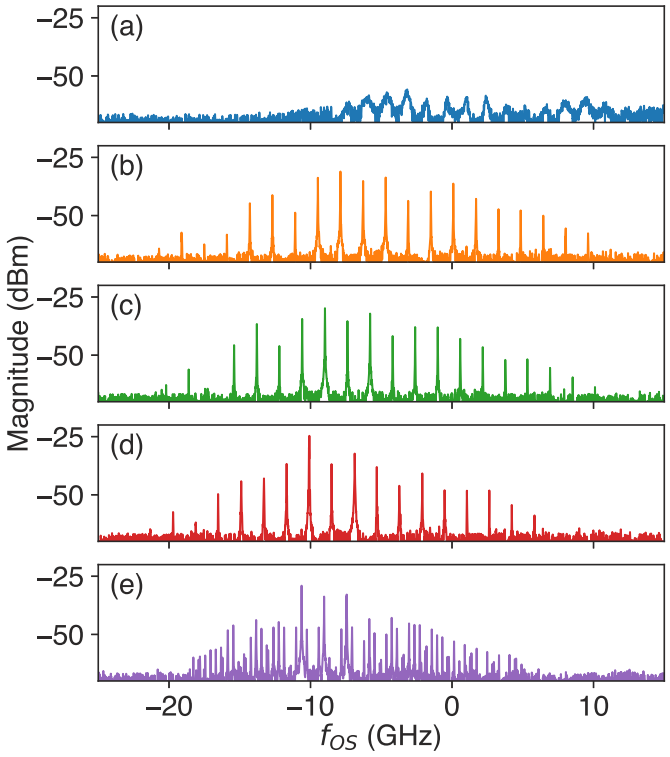

Fig. 4. Optical spectra corresponding to the QP and RP regimes in Fig. 3. The RP regime in (b–d) are distinctly marked by equidistant OFC lines featuring narrow linewidths, in contrast to the QP regime (a, e), which exhibits multiple secondary frequencies near each principal optical peak. The zeroth frequency corresponds to 194082.93 GHz.

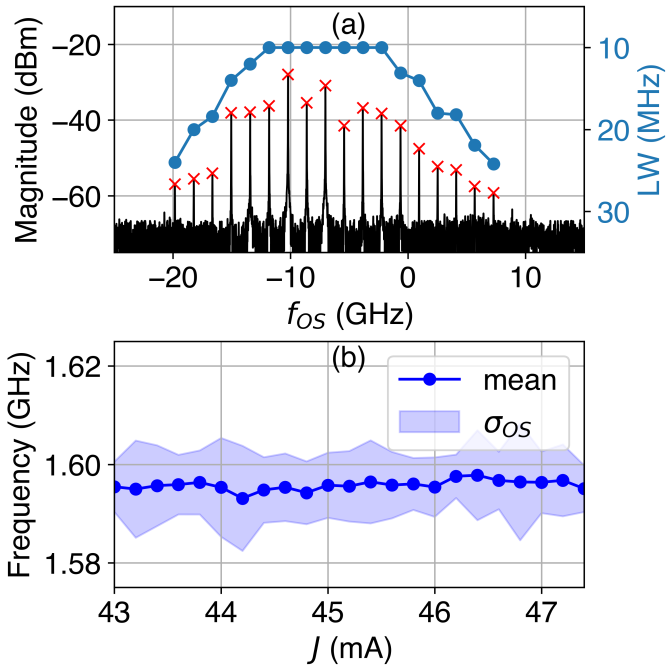

Fig. 5. Characterization of OFCs. (a) Optical spectra for $J = 47.20$ mA as a function of the optical detuning frequency, f_{OS} (measured with respect to the free-running LD) in the left vertical axis, and the 3-dB FWHM linewidths of each tooth plotted in blue in the right vertical axis. (b) Deviation of mode spacing from the mean as a function of J.

feedback that was introduced in [33]. In this work, the model was complemented to account for the intracavity field phase variation caused by the carrier density variation through the linewidth enhancement factor [37], [38]. The model is based on delay differential equations, and reads:

$$\dot{I}_C(t) = 2N(t)I_C(t) + \beta(t), \tag{1}$$

$$\dot{\varphi}(t) = \alpha N(t), \tag{2}$$

$$\dot{I}_{FH,i}(t) = -\tau_H{}^{-1} I_{FH,i}(t) + \dot{I}_{FH,i-1}(t), \tag{3}$$

$$\dot{I}_{FL,j}(t) = -\tau_L{}^{-1}(I_{FL,j}(t) - I_{FL,j-1}(t)), \tag{4}$$

$$\varepsilon^{-1}\dot{N}(t) = P + s\tanh(k\eta I_{FL,M}(t-\tau)) - N(t) - (1+2N(t))I_C(t). \tag{5}$$

The dot is for differentiation with respect to time t, which is normalized to the cavity photon lifetime τ_{ph}. $I_C(t)$ is the normalized intracavity intensity of the laser field; $\varphi(t)$ is the intracavity electrical field phase referenced to the laser frequency at the threshold; $N(t)$ is the normalized carrier density; ε is the ratio of the photon and carrier lifetimes; $\beta(t)$ is a white Gaussian noise source accounting for spontaneous emission with a variance of 10^{-10}; α is the linewidth enhancement factor; $P = (J/J_{th} - 1)/2$ is the pump parameter ($P = 0.0$ and $P = 0.5$ correspond to $J = J_{th}$ and $J = 2J_{th}$, respectively). Equations (3)-(4) describe multiple high- and low-pass filters in the feedback loop. $I_{FH,i}(t)$ ($I_{FL,j}(t)$) is the filtered electric signal after the high- (low-) pass filter, $i = 1,\ldots,K$ ($j = 1,\ldots,M$) accounts for the K-th (M-th) stage high- (low-) pass filtering [$I_{FH,0}(t) = I_C(t)$, $I_{FL,0}(t) = I_{FH,K}(t)$], and τ_H (τ_L) is the inverse of the cut-off frequency of the corresponding high- (low-) pass filter.

Nonlinearity of the time-delayed OE feedback caused by the saturation of the amplifiers is captured by the term $s\tanh[k\eta I_{FL,n}(t-\tau)]$ in Eq. (5) where η represents the feedback level, *i.e.*, the conversion coefficient of the intracavity intensity to an electrical signal, k is a small-signal amplification coefficient, and s defines the maximum amplitude of the feedback signal. The small η produces close-to-linear feedback, and when the signal amplitude is large, the term saturates with its value limited by s.

The following fixed parameters are used for the modeling, and were chosen to match experimental results: $\tau_{ph} = 1.26$ ps, $\varepsilon = 0.00126$, $\alpha = 1$, $\tau = 10.78$ ns, $\eta = 0.00085$, $s = 0.5$, $k = 2000$, $K = 4$, $M = 1$, $\tau_H^{-1} = 240$ MHz, and $\tau_L^{-1} = 10$ GHz.

As we reported previously for a similar system [30], the only steady-state solution of Eqs. (1–5) undergoes a sequence of Hopf bifurcations. It results in a set of the periodic pulsations which stabilize through torus bifurcations due to the Eckhaus mechanism (for more details, see [30]). The pulsations can be multistable and Fig. 6 demonstrates a sequence of switches between the pulsations with stepwise increase of the frequency with P. This frequency increase fits well by a square root function related to the free-running laser relaxation oscillation frequency, as was also demonstrated experimentally.

Like in the experiment, at $P \sim 0.4$ the sequence of switches is interrupted by a quasiperiodic state which, together with a similar state at $P \sim 0.5$, bounds a domain of the pump current where there exists a periodic regime with a frequency which is

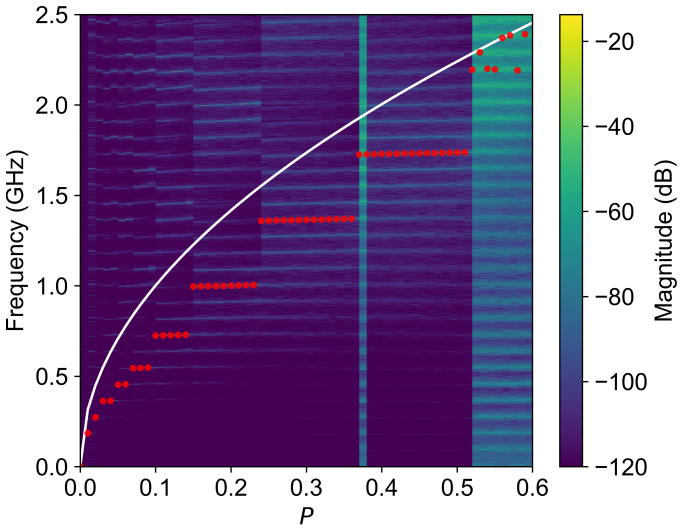

Fig. 6. Theoretical RF spectrograph of the laser intensity by varying P; maxima are highlighted in red at each P. The white curve is half the theoretical relaxation-oscillation frequency of the solitary LD, $\sqrt{8\varepsilon P - \varepsilon^2(1+2P)^2}/(8\pi)$.

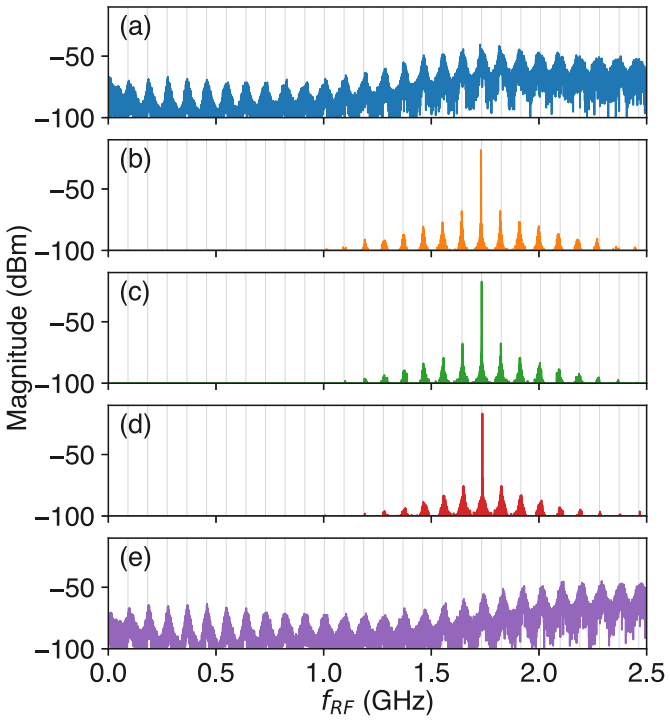

Fig. 7. Examples of the theoretical RF spectra from different parts of the Busse region in Fig. 6 observed between $P = 0.4$ and 0.52, at the following values of P: (a) 0.39; (b) 0.44; (c) 0.48; (d) 0.52; (e) 0.55. (a) and (e) exhibit characteristics of unstable periodic regime and broad spectral peaks. (b–d) display regular periodic limit cycles.

locked to a 19^{th} harmonic of the feedback loop's repetition rate $1/\tau$ (17^{th} in the experiment). The frequency and the character of the pulsations remain unchanged in the domain, which we interpret as a Busse balloon [35], [36]. Figure 7 (8) shows examples of RF (optical) spectra within the range $P \sim 0.4 - 0.5$ and clearly illustrates the stable character of the periodic pulsations in the stability domain bounded by instabilities.

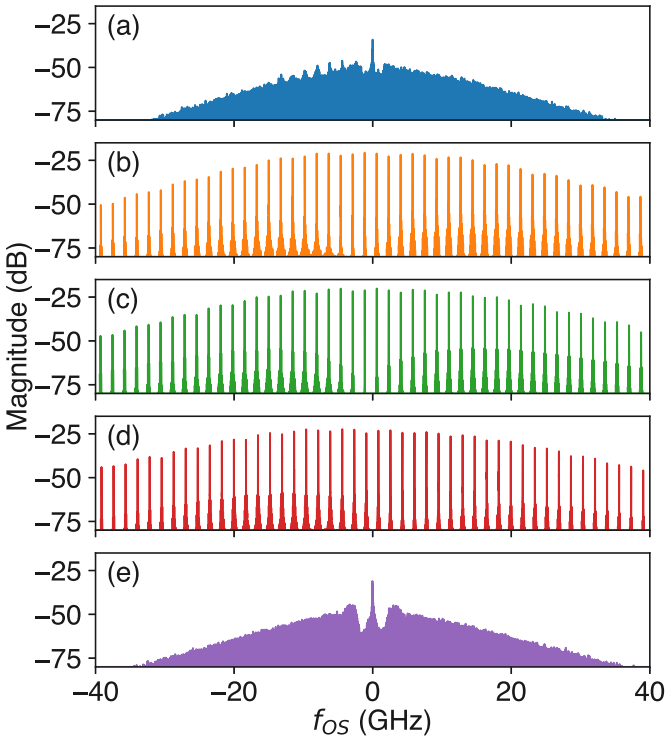

Fig. 8. Theoretical optical spectra corresponding to the regimes in Fig. 7 computed by the fast Fourier transform of the intracavity field complex amplitude $E(t) = \sqrt{I_C(t)}\exp(i\varphi(t))$.

The optical frequency combs are induced by the self-sustained periodic oscillations and corresponding intracavity field phase modulation due to the linewidth enhancement factor, characteristic of the semiconductor gain medium. A similar physical mechanism was previously reported in [15], [16] but for a semiconductor laser with external periodic modulation, and unlike feedback self-modulation of the pump current used in the present work. The inherent features of the system with delayed feedback are that the laser always oscillates at the frequency resonant with the feedback and the oscillation is stabilized within the Busse balloon providing optimal conditions for robust frequency comb generation without external signal sources.

IV. Conclusion

We experimentally demonstrate stable < 10 MHz linewidth OFC generation in a semiconductor LD subject to delayed nonlinear OE feedback. We find a range of the pump current J ($\sim 2J_{th}$) where the time-periodic optical output by the feedback remains stable with little change of the repetition rate. Under optimal conditions, a ~ 30 GHz width OFC preserves its shape and structure with ~ 1 % deviation of the line spacings from the mean over the full range of current variation. The optical span of 30 GHz is suitable for applications such as high-precision spectroscopy, broadband laser-based gas sensing, and molecular fingerprinting. The stability range is bounded by the quasiperiodic dynamics as demonstrated by the RF spectra.

A closed range of the stable RP regime with the constant frequency typically limited by a secondary bifurcation of

the Hopf type is commonly known as the Busse balloon, a concept originating in thermal fluid sciences [35], [36]. For the spatially extended systems, similar to a system with delayed feedback, the Busse balloon is defined as a domain with at least one stable heterogeneous periodic solution. In the modeling, based on the delay differential equations, we demonstrate the typical coexistence of multiple solutions for a range of J. The solutions are featured by a frequency being a n multiple ($n = 1, 2, 3...$) of the feedback delay τ. It confirms the experimental observation of the stable OFC with ~ 1.60 GHz spacing which is 17 times the feedback loop's repetition rate τ^{-1}.

Acknowledgment

The work of A.V.K., G.O.D., and E.A.V. was supported by the Ministry of Education and Science of the Russian Federation (research project No. 2019-1442). A.L., D.S.C., and M.S.I. acknowledge the financial support of the Conseil Régional Grand Est.

References

[1] F. Adler, P. Masłowski, A. Foltynowicz, K. C. Cossel, T. C. Briles, I. Hartl, and J. Ye, "Mid-infrared fourier transform spectroscopy with a broadband frequency comb," *Optics express*, vol. 18, no. 21, pp. 21 861–21 872, 2010.

[2] J. Mandon, G. Guelachvili, and N. Picqué, "Fourier transform spectroscopy with a laser frequency comb," *Nature Photonics*, vol. 3, no. 2, pp. 99–102, 2009.

[3] S. A. Diddams, D. J. Jones, J. Ye, S. T. Cundiff, J. L. Hall, J. K. Ranka, R. S. Windeler, R. Holzwarth, T. Udem, and T. W. Hänsch, "Direct link between microwave and optical frequencies with a 300 thz femtosecond laser comb," *Physical review letters*, vol. 84, no. 22, p. 5102, 2000.

[4] M. J. Thorpe, K. D. Moll, R. J. Jones, B. Safdi, and J. Ye, "Broadband cavity ringdown spectroscopy for sensitive and rapid molecular detection," *Science*, vol. 311, no. 5767, pp. 1595–1599, 2006.

[5] S. A. Diddams, L. Hollberg, and V. Mbele, "Molecular fingerprinting with the resolved modes of a femtosecond laser frequency comb," *Nature*, vol. 445, no. 7128, pp. 627–630, 2007.

[6] P. Del'Haye, A. Schliesser, O. Arcizet, T. Wilken, R. Holzwarth, and T. J. Kippenberg, "Optical frequency comb generation from a monolithic microresonator," *Nature*, vol. 450, no. 7173, pp. 1214–1217, 2007.

[7] E. A. Anashkina, M. P. Marisova, A. V. Andrianov, R. A. Akhmedzhanov, R. Murnieks, M. D. Tokman, L. Skladova, I. V. Oladyshkin, T. Salgals, I. Lyashuk *et al.*, "Microsphere-based optical frequency comb generator for 200 ghz spaced wdm data transmission system," in *Photonics*, vol. 7, no. 3. Multidisciplinary Digital Publishing Institute, 2020, p. 72.

[8] R. Ullah, S. Ullah, G. Z. Khan, Y. Mao, J. Ren, J. Zhao, S. Chen, M. Li, and J. Khan, "Ultrawide and tunable self-oscillating optical frequency comb generator based on an optoelectronic oscillator," *Results in Physics*, vol. 22, p. 103849, 2021.

[9] J. Kim and Y. Song, "Ultralow-noise mode-locked fiber lasers and frequency combs: principles, status, and applications," *Advances in Optics and Photonics*, vol. 8, no. 3, pp. 465–540, 2016.

[10] C. D. Muñoz, M. Varón, F. Destic, and A. Rissons, "Self-starting vcsel-based optical frequency comb generator," *Optics Express*, vol. 28, no. 23, pp. 34 860–34 874, 2020.

[11] A. Quirce, C. de Dios, A. Valle, L. Pesquera, and P. Acedo, "Polarization dynamics in vcsel-based gain switching optical frequency combs," *Journal of Lightwave Technology*, vol. 36, no. 10, pp. 1798–1806, 2018.

[12] V. Sharma, S. Singh, E. A. Anashkina, and A. V. Andrianov, "Optical frequency comb generation by the exploitation of gain modulation phenomenon in semiconductor optical amplifier," *Optical Engineering*, vol. 60, no. 6, pp. 066 108–066 108, 2021.

[13] J. Li, J. Zheng, T. Pu, H. Zhou, X. Zhang, Y. Li, and H. Zhu, "A simple optical frequency comb generator based on the monolithic integrated dual-tone semiconductor laser subject to the gain-switching effect," in *2021 19th International Conference on Optical Communications and Networks (ICOCN)*. IEEE, 2021, pp. 01–03.

[14] D. Citrin, "Connection between optical frequency combs and microwave frequency combs produced by active-mode-locked lasers subject to timing jitter," *Physical Review Applied*, vol. 16, no. 1, p. 014004, 2021.

[15] A. Rosado, E. P. Martin, A. Pérez-Serrano, J. M. G. Tijero, I. Esquivias, and P. M. Anandarajah, "Optical frequency comb generation via pulsed gain-switching in externally-injected semiconductor lasers using step-recovery diodes," *Optics & Laser Technology*, vol. 131, p. 106392, 2020. [Online]. Available: https://www.sciencedirect.com/science/article/pii/S0030399220310252

[16] Y. Fan, K. Li, P. Li, B. Copner, and N. J. Copner, "Linewidth sharpening in optical frequency combs via a gain switched semiconductor laser with external optical feedback," *Journal of Lightwave Technology*, vol. 39, no. 1, pp. 105–111, 2021.

[17] G. Millot, S. Pitois, M. Yan, T. Hovhannisyan, A. Bendahmane, T. W. Hänsch, and N. Picqué, "Frequency-agile dual-comb spectroscopy," *Nature Photonics*, vol. 10, no. 1, pp. 27–30, 2016. [Online]. Available: https://doi.org/10.1038/nphoton.2015.250

[18] P. Ho, L. A. Glasser, E. P. Ippen, and H. A. Haus, "Picosecond pulse generation with a cw GaAlAs laser diode," *Applied Physics Letters*, vol. 33, no. 3, pp. 241–242, 08 1978. [Online]. Available: https://doi.org/10.1063/1.90312

[19] A. Pasquazi, M. Peccianti, L. Razzari, D. J. Moss, S. Coen, M. Erkintalo, Y. K. Chembo, T. Hansson, S. Wabnitz, P. Del'Haye, X. Xue, A. M. Weiner, and R. Morandotti, "Micro-combs: A novel generation of optical sources," *Physics Reports*, vol. 729, pp. 1–81, 2018, micro-combs: A novel generation of optical sources. [Online]. Available: https://www.sciencedirect.com/science/article/pii/S0370157317303253

[20] J.-M. Liu and S. Tang, "Chaotic communications using synchronized semiconductor lasers with optoelectronic feedback," *Comptes Rendus Physique*, vol. 5, no. 6, pp. 657–668, 2004.

[21] J. Wang, J. Yu, W. Miao, B. Sun, S. Jia, W. Wang, and Q. Wu, "Long-range, high-precision absolute distance measurement based on two optoelectronic oscillators," *Optics Letters*, vol. 39, no. 15, pp. 4412–4415, 2014.

[22] V. K. Khanna, "Existing and emerging detection technologies for dna (deoxyribonucleic acid) finger printing, sequencing, bio-and analytical chips: A multidisciplinary development unifying molecular biology, chemical and electronics engineering," *Biotechnology advances*, vol. 25, no. 1, pp. 85–98, 2007.

[23] S. Tang and J. Liu, "Chaotic pulsing and quasi-periodic route to chaos in a semiconductor laser with delayed opto-electronic feedback," *IEEE journal of quantum electronics*, vol. 37, no. 3, pp. 329–336, 2001.

[24] H. D. Abarbanel, M. B. Kennel, L. Illing, S. Tang, H. Chen, and J. Liu, "Synchronization and communication using semiconductor lasers with optoelectronic feedback," *IEEE journal of quantum electronics*, vol. 37, no. 10, pp. 1301–1311, 2001.

[25] F.-Y. Lin and J.-M. Liu, "Nonlinear dynamics of a semiconductor laser with delayed negative optoelectronic feedback," *IEEE journal of quantum electronics*, vol. 39, no. 4, pp. 562–568, 2003.

[26] F. Lin and J. Liu, "Harmonic frequency locking in a semiconductor laser with delayed negative optoelectronic feedback," *Applied physics letters*, vol. 81, no. 17, pp. 3128–3130, 2002.

[27] G.-Q. Xia, S.-C. Chan, and J.-M. Liu, "Multistability in a semiconductor laser with optoelectronic feedback," *Optics Express*, vol. 15, no. 2, pp. 572–576, 2007.

[28] S.-C. Chan, G.-Q. Xia, and J.-M. Liu, "Optical generation of a precise microwave frequency comb by harmonic frequency locking," *Optics letters*, vol. 32, no. 13, pp. 1917–1919, 2007.

[29] M. S. Islam, A. V. Kovalev, E. A. Viktorov, D. S. Citrin, and A. Locquet, "Microwave Frequency Comb Generation by Gain-Switching Versus Relaxation Oscillations," *IEEE Photonics Technology Letters*, vol. 33, no. 10, pp. 491–494, 2021.

[30] M. S. Islam, A. Kovalev, G. Coget, E. Viktorov, D. Citrin, and A. Locquet, "Staircase dynamics of a photonic microwave oscillator based on a laser diode with delayed optoelectronic feedback," *Physical Review Applied*, vol. 13, no. 6, p. 064038, 2020.

[31] B. Buscaino, M. Zhang, M. Lončar, and J. M. Kahn, "Design of efficient resonator-enhanced electro-optic frequency comb generators," *Journal of Lightwave Technology*, vol. 38, no. 6, pp. 1400–1413, 2020.

[32] M. J. Wishon, D. Choi, T. Niebur, N. Webster, Y. K. Chembo, E. A. Viktorov, D. S. Citrin, and A. Locquet, "Low-noise X-band Tunable Microwave Generator Based on a Semiconductor Laser with Feedback," *IEEE Photon. Technol. Lett.*, vol. 30, no. 18, pp. 1597–1600, 2018.

[33] M. S. Islam, A. V. Kovalev, E. A. Viktorov, D. S. Citrin, and A. Locquet, "Optical square-wave generation in a semiconductor laser with optoelectronic feedback," *Opt. Lett.*, vol. 46, no. 24, pp.

6031–6034, Dec 2021. [Online]. Available: https://opg.optica.org/ol/abstract.cfm?URI=ol-46-24-6031

[34] M. S. Islam, A. V. Kovalev, V. N. Iachkula, E. A. Viktorov, D. S. Citrin, and A. Locquet, "Doublet structure in the optical spectrum of a semiconductor laser with optoelectronic feedback in a square-wave regime," *Applied Physics Letters*, vol. 121, no. 26, p. 261101, 12 2022. [Online]. Available: https://doi.org/10.1063/5.0127719

[35] F. H. Busse, "On the stability of two-dimensional convection in a layer heated from below," *Journal of Mathematics and Physics*, vol. 46, no. 1-4, pp. 140–150, 1967. [Online]. Available: https://onlinelibrary.wiley.com/doi/abs/10.1002/sapm1967461140

[36] ——, "Non-linear properties of thermal convection," *Reports on Progress in Physics*, vol. 41, no. 12, p. 1929, dec 1978. [Online]. Available: https://dx.doi.org/10.1088/0034-4885/41/12/003

[37] C. Henry, "Theory of the linewidth of semiconductor lasers," *IEEE J. Quantum Electron.*, vol. 18, p. 259, 1982.

[38] G. H. M. van Tartwijk and D. Lenstra, "Semiconductor lasers with optical injection and feedback," *Quantum and Semiclassical Optics: Journal of the European Optical Society Part B*, vol. 7, no. 2, p. 87, apr 1995. [Online]. Available: https://dx.doi.org/10.1088/1355-5111/7/2/003